

Characterization of the acid sites in dealuminated nanosized HZSM-5 zeolite with the probe molecule trimethylphosphine

Weiping Zhang*, Xiuwen Han, Xiumei Liu, Xinhe Bao¹

State Key Laboratory of Catalysis, Dalian Institute of Chemical Physics, Chinese Academy of Sciences, Dalian 116023, China

Received 6 June 2002; received in revised form 30 July 2002; accepted 30 July 2002

Abstract

The acid sites in dealuminated HZSM-5 zeolite with crystal sizes down to the nanoscale were firstly characterized by the probe molecule trimethylphosphine (TMP). As evidenced by the combination of ³¹P CP/MAS NMR, ²⁷Al MAS and ¹H → ²⁷Al CP/MAS NMR measurements, the Brønsted acid sites of both microsized and nanosized HZSM-5 could be decreased upon the dealumination of zeolitic framework after hydrothermal treatment. At the same time, the appearance of Lewis acid sites was observed. The dealuminated nanosized HZSM-5 is easier to form Lewis acid sites than microsized HZSM-5, and the type of Lewis acid sites in nanosized HSM-5 is more than one. In addition, the origin of Lewis acid sites is mainly associated with the aluminum at ca. 30 ppm in the ²⁷Al MAS NMR spectra, and only a part of which in the dealuminated HZSM-5 zeolite acts as Lewis acid sites.

© 2002 Elsevier Science B.V. All rights reserved.

Keywords: Nanosized HZSM-5 zeolite; Trimethylphosphine (TMP); Hydrothermal dealumination; ³¹P MAS NMR; Lewis acid; Probe molecule

1. Introduction

Acidity is an important topic in the field of zeolite research. A number of papers in the literature reported that dealumination of zeolite can enhance its activity in the acid-catalyzed reactions [1–5]. Most authors ascribed this to the existence of Lewis acid sites with the combination of Brønsted acid sites after dealumination of zeolite [6–8]. They employed a lot of methods to characterize the acidity in solid cata-

lysts [9]. Among them, the infrared spectroscopy of adsorbed pyridine has been used extensively to provide evidence for both Brønsted and Lewis acid sites [9]. However, the limitation of this technique lies in the difficulty to determine the strength of the acidity and the number of acid sites in a quantitative way for the different extinction coefficients of each adsorbed species. Trimethylphosphine has emerged as a promising approach to characterize the acid sites in zeolites [10–12] and other materials [13–15] using ³¹P MAS NMR spectroscopy. Trimethylphosphine (TMP) is suitable for ³¹P MAS NMR studies as it has isotope of 100% natural abundance, nuclear spin of 1/2, and large gyromagnetic ratio. Moreover, TMP has rather smaller size of about 5.5 Å [16]. It is small enough to fit into the cavities or channels of many zeolites, including ZSM-5. However, the acidity of dealuminated

* Corresponding author. Present address: Steacie Institute for Molecular Sciences, National Research Council of Canada, 100 Sussex Drive, Ottawa, Ont., Canada K1A 0R6.

Tel.: +1-613-990-3405; fax: +1-613-998-7833.

E-mail addresses: weiping.zhang@nrc.ca (W. Zhang),

xhbao@dicp.ac.cn (X. Bao).

¹ Co-corresponding author.

HZSM-5 zeolite has not been well investigated using TMP as the probe molecule in the literature. In our previous papers, we studied the microporous structure [17] and stability [18] of nanosized HZSM-5 zeolite. Here, we focus on the acidity variations of hydrothermally dealuminated HZSM-5 zeolite with crystal sizes down to the nanoscale by ^{31}P MAS NMR of adsorbed TMP. The origin of Lewis acid site is also discussed.

2. Experimental

2.1. Sample preparation

The starting HZSM-5 samples ($\text{Si}/\text{Al} = 28$) with the crystal sizes of 1000 and 70 nm, respectively were prepared according to a procedure published in our previous papers [19,20]. They were obtained by deammonium at 500 °C for 5 h and denoted as *micro*-HZ and *nano*-HZ, respectively. Dealumination by steaming at 400, 500, 700 °C were described in detail in our preceding study [18].

2.2. NMR measurement

A special device was designed by us to carry out the on-line treatment of zeolite samples [21,22]. In this apparatus, zeolites were dehydrated typically at 673 K and at a pressure below 10^{-2} Pa for 10–20 h before adsorption. After dehydration, 100 Torr trimethylphosphine (Acros Organics) was introduced and kept for 30 min at room temperature, then degassing it at 323 K for 10–15 min to remove most physical adsorbates from the surface [14]. Finally, the samples were filled in situ into an NMR rotor, sealed, and transferred to the spectrometer without exposure to air. Such dealing with the samples can avoid oxidation of TMP and also its toxicity.

NMR spectra were recorded at room temperature on a Bruker DRX-400 spectrometer with a BBO MAS probe using 4 mm ZrO_2 rotors. ^{31}P MAS NMR spectra with high-power proton decoupling were collected at 161.9 MHz, using a $\pi/6$ pulse of 2 μs and recycle delay of 2 s. Samples were spun at 5 kHz, and chemical shifts were referenced to 85% H_3PO_4 . In order to compare quantitatively, all the ^{31}P MAS NMR spectra were acquired under the same NMR conditions and the

same number of 1600 scans, and drawn with the correction of sample mass. ^{27}Al MAS NMR spectra were collected at 104.3 MHz using a 0.75 μs $\pi/12$ pulse with a 3 s recycle delay and 600 scans. $^1\text{H} \rightarrow ^{27}\text{Al}$ CP/MAS spectra were recorded with a single contact, an optimized contact time of 1.2 ms, a recycle delay of 3 s, and 10,000–20,000 scans. The Hartmann-Hahn condition was established as described in our previous paper [20]. ^{27}Al NMR spectra were recorded with samples spun at 10 kHz, and chemical shifts were referenced to 1% aqueous $\text{Al}(\text{H}_2\text{O})_6^{3+}$.

3. Results

3.1. ^{31}P MAS NMR

The ^{31}P MAS NMR spectra of micro-sized and nanosized HZSM-5 before and after hydrothermal dealumination are shown in Figs. 1 and 2, respectively. The resonance at -4.5 ppm is ascribed to the protonated adduct TMPH^+ , i.e. the reaction of TMP with the Brönsted acid sites. The major resonance at -57 and -60 ppm are assigned to the Lewis-bound TMP adducts [12,16]. Moreover, there is also a little physically adsorbed TMP at -62.1 ppm. In order to display more clearly the effects of hydrothermal treatment on the variations of Lewis acid sites, the peaks at high field were deconvoluted quantitatively using fitted Gaussian-Lorentzian line shapes (see Figs. 1 and 2). With increasing steaming temperature, the peak intensity of Brönsted acid sites in both micro-sized and nanosized HZSM-5 decreased, and the amount of Lewis acid sites at -60 ppm increased when dealuminated at 400 °C, but decreased at higher steaming temperatures. In addition, for the nanosized HZSM-5, another type of Lewis acid site appeared at -57 ppm besides that at -60 ppm. Its peak intensity also varied as that at -60 ppm after dealumination. The spinning sidebands are clearly seen in the spectra of both micro-sized and nanosized HZSM-5, which indicates that the motion of TMP is severely restricted in ZSM-5 channels for they have nearly the same diameter [16].

3.2. ^{27}Al MAS NMR and $^1\text{H} \rightarrow ^{27}\text{Al}$ CP/MAS NMR

Fig. 3 shows the ^{27}Al MAS NMR spectra of dealuminated micro-sized and nanosized HZSM-5 before

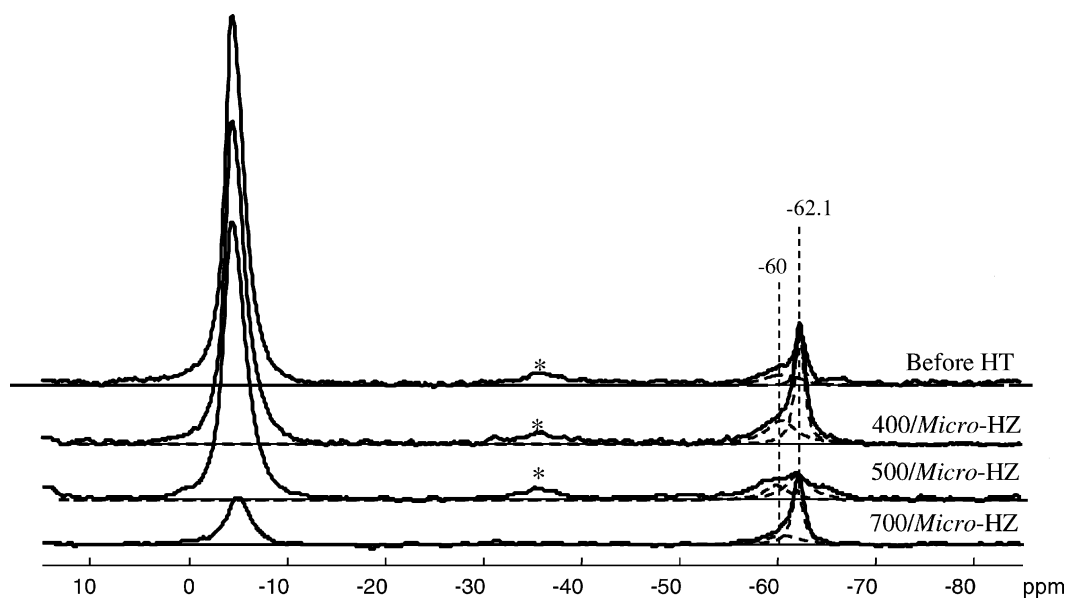


Fig. 1. ^{31}P MAS NMR spectra of $(\text{CH}_3)_3\text{P}$ in micro-sized HZSM-5 hydrothermally treated at different temperatures (with proton decoupling); the symbol * denotes the spinning sidebands.

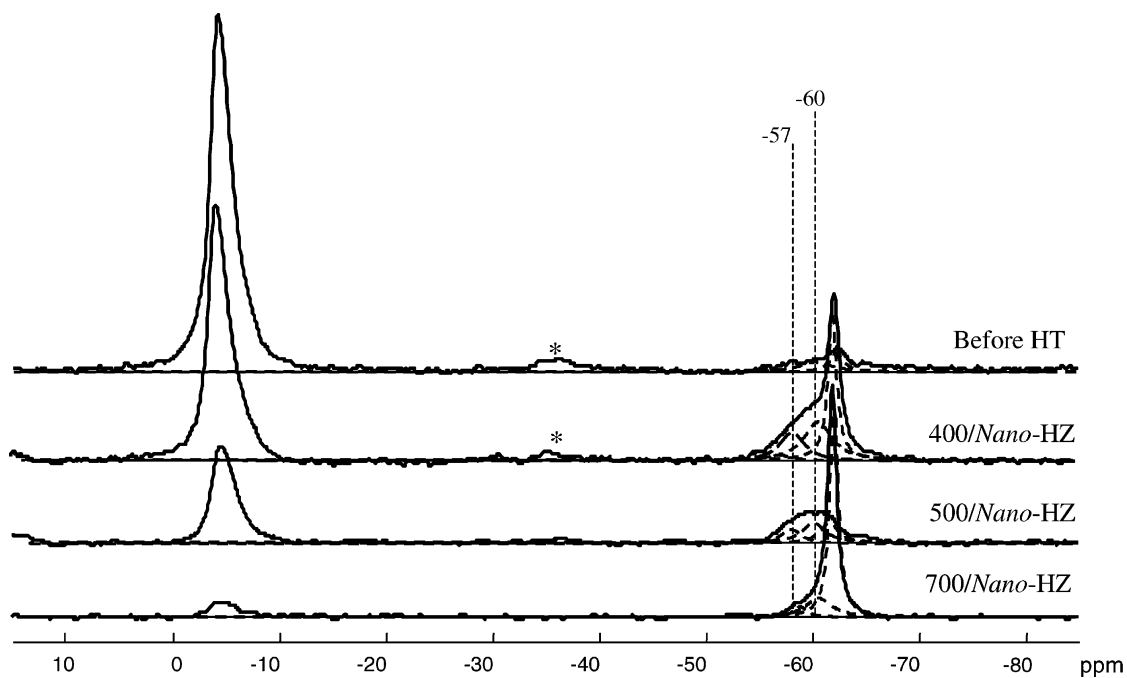


Fig. 2. ^{31}P MAS NMR spectra of $(\text{CH}_3)_3\text{P}$ in nano-sized HZSM-5 hydrothermally treated at different temperatures (with proton decoupling); the symbol * denotes the spinning sidebands.

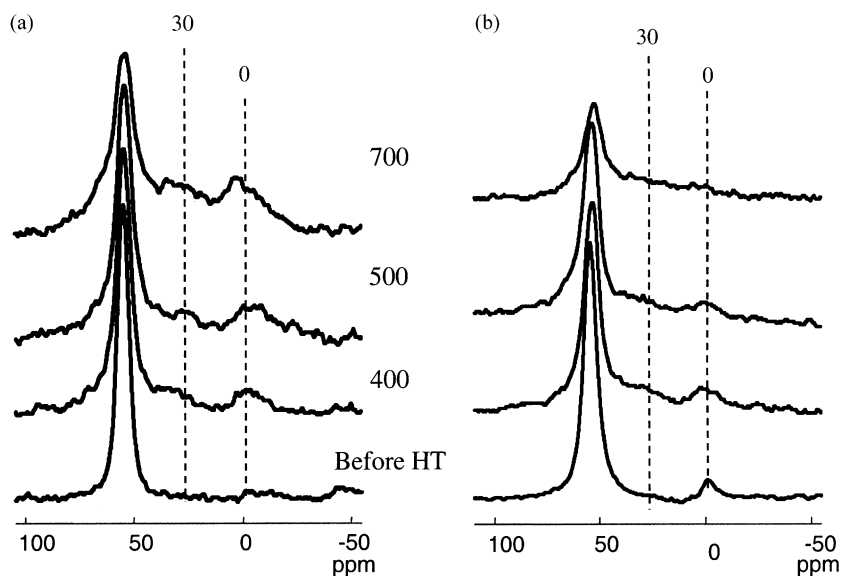


Fig. 3. ^{27}Al MAS NMR spectra of microsized (a) and nanosized (b) HZSM-5 zeolite hydrothermally treated at different temperatures (without adsorption of TMP).

adsorption of TMP. There are two main peaks as expected. One at 52 ppm is typically assigned to the tetrahedral framework Al, and the other at 0 ppm is attributed to octahedral nonframework Al [18–20]. In addition, a broad signal centered at ca. 30 ppm also appeared after dealumination, which may be

ascribed to the pentacoordinated nonframework Al [23] or distorted four-coordinated Al [24]. With the increase of steaming temperature, the peak intensity of the framework Al of the nanosized HZSM-5 decreases more readily than that of the microsized HZSM-5. Both the aluminum at ca. 30 and 0 ppm are

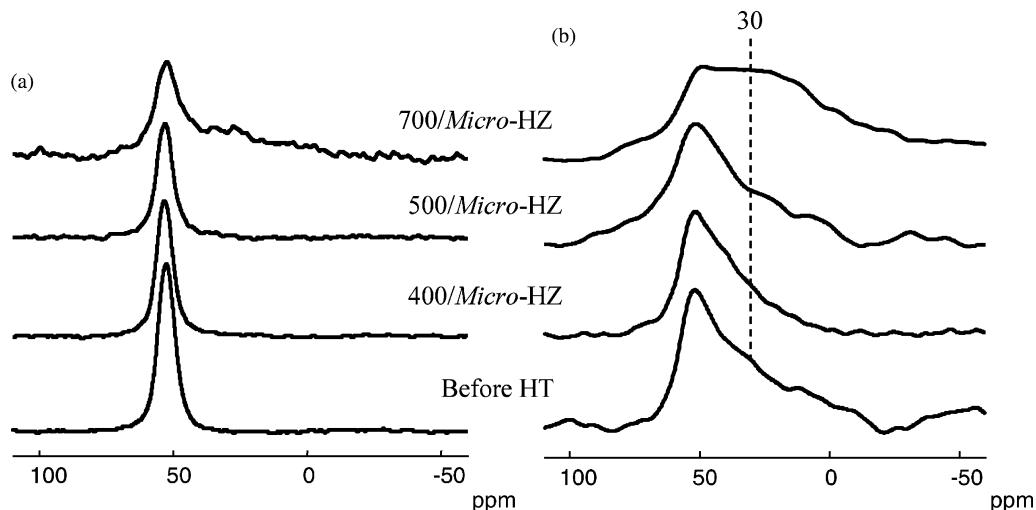


Fig. 4. ^{27}Al MAS (a) and $^1\text{H} \rightarrow ^{27}\text{Al}$ CP/MAS NMR (b) spectra of dealuminated microsized HZSM-5 after dehydration and adsorption of TMP.

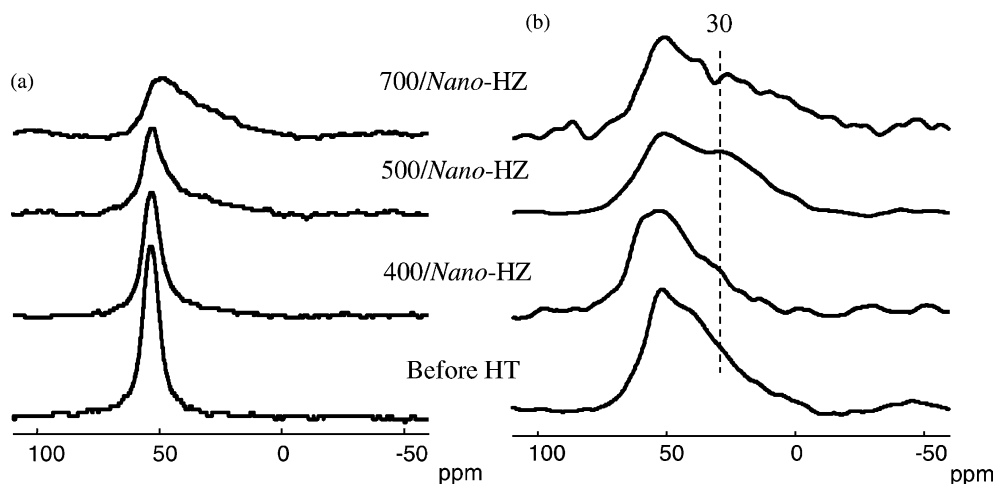


Fig. 5. ^{27}Al MAS (a) and $^1\text{H} \rightarrow ^{27}\text{Al}$ CP/MAS NMR (b) spectra of dealuminated nanosized HZSM-5 after dehydration and adsorption of TMP.

observed in the ^{27}Al MAS NMR spectra of microsized and nanosized HZSM-5 after dealumination. While for the nanosized HZSM-5 steamed after 700 °C, the signal at 0 ppm is gone and that at ca. 30 ppm becomes much broadening. This may be due to the larger increase of the quadrupolar interaction between the Al atoms at ca. 30 ppm after hydrothermal treatment.

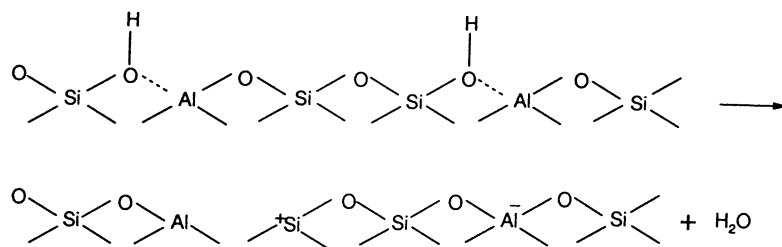
After dehydration and adsorption of TMP, ^{27}Al MAS NMR and $^1\text{H} \rightarrow ^{27}\text{Al}$ CP/MAS NMR spectra of dealuminated microsized and nanosized HZSM-5 are displayed in Figs. 4 and 5, respectively. It is clear that only the framework Al at 52 ppm and aluminum at ca. 30 ppm can be observed in the ^{27}Al MAS NMR spectra of both the dealuminated microsized and nanosized HZSM-5. After cross polarization, only the signal at ca. 30 ppm are increased. Nearly no signal of nonframework Al at 0 ppm can be detected compared with the corresponding ^{27}Al MAS NMR spectra in Fig. 3 before adsorption of TMP.

4. Discussion

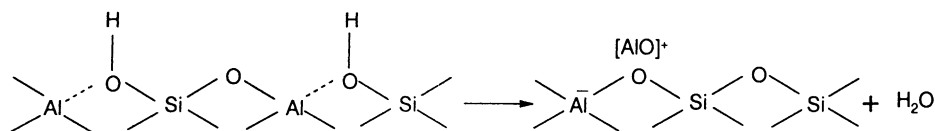
The results of ^{31}P MAS NMR quantitative study show that after hydrothermal treatment the amount of Brønsted acid sites on both the microsized and nanosized HZSM-5 decreased, which is consistent with our previous ^1H MAS NMR study [18], i.e. the peak intensity of Brønsted sites at 3.9 ppm in their

corresponding ^1H MAS NMR spectra also decreased. From the results of ^{27}Al MAS NMR spectra (Fig. 3), obvious dealumination from the zeolitic framework is observed after steaming treatment. So the decrease of Brønsted acid sites is mainly due to the dealumination of the zeolitic framework. After dealumination, there appeared Lewis acid sites in samples, but in the ^{31}P MAS NMR spectra there are two kinds of Lewis acid sites in the dealuminated nanosized HZSM-5 at -57 and -60 ppm, respectively. While for the dealuminated microsized HZSM-5, there is one type of Lewis acid site at -60 ppm. Moreover, under the same steaming conditions, the amount of Lewis acid sites in dealuminated nanosized HZSM-5 is more than that in dealuminated microsized HZSM-5. Thus, nanosized HZSM-5 is easier to form the Lewis acid sites than microsized HZSM-5 after hydrothermal treatment.

Many authors observed the formation of Lewis acid site after dealumination of zeolites [10–16], but different opinions on the origin of Lewis acid site were reported in the literature. In general, there are two typical models. One is by Uytterhoeven et al. [25] (see in Scheme 1). They thought that the bridged hydroxyls on the zeolitic framework dehydrated to form the tricoordinated framework aluminum as the Lewis acid site, at the same time no dealumination of the zeolitic framework took place. The other is by Jacobs and Beyer [26] (see in Scheme 2). They considered the nonframework Al like $[\text{Al}-\text{O}]^+$ from dealumination



Scheme 1.



Scheme 2.

of zeolitic framework as the Lewis acid site, i.e. Lewis acid site is associated with the nonframework Al.

However, no tricoordinated framework Al was observed by the ^{27}Al MAS NMR spectra [27,28] and also by the X-ray fluorescence (XRF) [29]. So Uytterhoeven model is not accepted extensively so far. We and other authors [7,30] tend to accept the Jacobs model. In the ^{27}Al MAS NMR spectra, we find the increase of nonframework Al upon hydrothermal treatment. But in the corresponding ^{31}P MAS NMR spectra, the amount of Lewis acid site does not increase obviously. On the contrary, it decreases at higher steaming temperatures. This is due to the condensation of nonframework aluminum hydroxyls to polymeric aluminum species [30,31]. As demonstrated in our previous ^1H MAS NMR study [18], the peak intensity of nonframework AlOH at 2.7 ppm decreased clearly after hydrothermal treatment, which also supports above explanation. Thus, only a part of nonframework aluminum forms the Lewis acid sites after dealumination.

However, which kind of nonframework aluminum is associated with the Lewis acid site? Is that at ca. 30 or 0 ppm in the ^{27}Al MAS NMR spectra? Comparing with the results of ^{27}Al MAS NMR study in the dealuminated microsized and nanosized HZSM-5 before and after adsorption of TMP (see Figs. 3, 4a and 5a), not the signal at 0 ppm but the signal at ca. 30 ppm appeared in the ^{27}Al MAS NMR spectra after adsorption of TMP. This proves that TMP molecules may

not be adsorbed by the nonframework aluminum at 0 ppm after dehydration. So the coordination number around this site is not six any longer, which results in too larger quadrupolar effect to be detected. Therefore, only the aluminum at ca. 30 ppm may adsorb TMP after dehydration. The magnetic vector of hydrogen atoms in the methyls of TMP can be transferred to the neighboring aluminum atom by the $^1\text{H} \rightarrow ^{27}\text{Al}$ cross polarization technique. So we observed the signal enhancement at ca. 30 ppm in the $^1\text{H} \rightarrow ^{27}\text{Al}$ CP/MAS NMR spectra (see Figs. 4b and 5b). These facts reveal that the Lewis acid site is associated with the aluminum at ca. 30 ppm. Similar result was obtained by Chen et al. in characterizing transition aluminas [32]. In Fig. 2, we observed two types of Lewis acid sites in the dealuminated nanosized HZSM-5. This might be due to the existence of two types of nonframework Al (pentacoordinated and distorted four-coordinated Al) in such samples. However, based on the results from above ^{27}Al and ^{31}P MAS NMR, the amount of Lewis acid sites does not increase with the increasing nonframework aluminum at ca. 30 ppm. As discussed above, this is due to the fact that only a part of the aluminum at ca. 30 ppm acts as Lewis acid sites.

5. Conclusions

The Brønsted acid sites in both the microsized and nanosized HZSM-5 decreased after dealumination by

hydrothermal treatment. Compared with dealuminated microsized HZSM-5, nanosized HZSM-5 is much easier to form Lewis acid sites, the type of which is more than one. The Lewis acid sites mainly derive from the aluminum at ca. 30 ppm in the ^{27}Al MAS NMR spectra. In addition, only a part of this kind of aluminum acts as Lewis acid sites.

Acknowledgements

We are grateful for the support of the National Natural Science Foundation of China and the Ministry of Science and Technology of China through the 973 Project. We also thank Prof. Xiangsheng Wang and Dr. Xinwen Guo of Dalian University of Technology for their kindly providing zeolite samples.

References

- [1] N.Y. Topsoe, F. Joensen, E.G. Derouane, *J. Catal.* 110 (1988) 404.
- [2] D.B. Lukyanov, *Zeolites* 11 (1991) 325.
- [3] D.B. Lukyanov, *Zeolites* 14 (1994) 233.
- [4] J. Datka, S. Marschmeyer, T. Neubauer, J. Meusinger, H. Papp, F.W. Schütze, I. Szpyt, *J. Phys. Chem.* 100 (1996) 14451.
- [5] S. Kumar, A.K. Sinha, S.G. Hegde, S. Sivasanker, *J. Mol. Catal. A* 154 (2000) 115.
- [6] R.M. Lago, W.O. Haag, R.J. Mikowsky, D.H. Oslon, S.D. Hellring, K.D. Schmitt, G.T. Kerr, in: Y. Murakami, et al. (Eds.), *Proceedings of the 7th International Zeolite Conference, Kondansha, Tokyo, 1986*, p. 677.
- [7] R.A. Beyerlein, C. ChoiFeng, J.B. Hall, B.J. Huggins, G.J. Ray, *Top. Catal.* 4 (1997) 27.
- [8] M.A. Kuehne, H.H. Kung, J.T. Miller, *J. Catal.* 171 (1997) 293.
- [9] J.A. Lercher, C. Gründling, G. Eder-Mirth, *Catal. Today* 27 (1996) 353.
- [10] J.H. Lunsford, W.P. Rothwell, W. Shen, *J. Am. Chem. Soc.* 107 (1985) 1540.
- [11] A. Bendada, E.F. DeRose, J.J. Fripiat, *J. Phys. Chem.* 98 (1994) 3838.
- [12] H.M. Kao, C.P. Grey, *Chem. Phys. Lett.* 259 (1996) 459.
- [13] L. Baltusis, J.S. Frye, G.E. Maciel, *J. Am. Chem. Soc.* 109 (1987) 40.
- [14] D. Coster, A. Bendada, F.R. Chen, J.J. Fripiat, *J. Catal.* 140 (1993) 497.
- [15] T.C. Sheng, I.D. Gay, *J. Catal.* 145 (1994) 10.
- [16] J.H. Lunsford, *Top. Catal.* 4 (1997) 91.
- [17] W. Zhang, X. Han, X. Liu, H. Lei, X. Bao, *Chem. Commun.* (2001) 293;
W. Zhang, X. Han, X. Liu, H. Lei, X. Liu, X. Bao, *Microporous Mesoporous Mater.* 53 (2002) 145.
- [18] W. Zhang, X. Han, X. Liu, X. Bao, *Microporous Mesoporous Mater.* 50 (2001) 13.
- [19] W. Zhang, X. Bao, X. Guo, X. Wang, *Catal. Lett.* 60 (1999) 89.
- [20] W. Zhang, D. Ma, X. Han, X. Liu, X. Bao, X. Guo, X. Wang, *J. Catal.* 188 (1999) 393.
- [21] W. Zhang, D. Ma, X. Liu, X. Liu, X. Bao, *Chem. Commun.* (1999) 1091.
- [22] D. Ma, Y. Shu, W. Zhang, X. Han, Y. Xu, X. Bao, *Angew. Chem. Int. Ed.* 39 (2000) 2928;
D. Ma, Y. Shu, W. Zhang, X. Han, Y. Xu, X. Bao, *Angew. Chem.* 112 (2000) 3050.
- [23] L.B. Alemany, G.W. Kirker, *J. Am. Chem. Soc.* 108 (1986) 6158;
J. Rocha, S.W. Carr, J. Klinowski, *Chem. Phys. Lett.* 187 (1991) 401.
- [24] T.H. Chen, B.H. Wouters, P.J. Grobet, *Eur. J. Inorg. Chem.* (2000) 281;
J.A. Van Bokhoven, A.L. Roest, D.C. Koningsberger, J.T. Miller, A.P.M. Kentgens, *J. Phys. Chem. B* 104 (2000) 6743.
- [25] J.B. Uytterhoeven, L.G. Christner, W.K. Hall, *J. Phys. Chem.* 69 (1965) 2117.
- [26] P. Jacobs, H.K. Beyer, *J. Phys. Chem.* 83 (1979) 1174.
- [27] D. Freude, T. Frohlich, H. Pfeifer, G. Scheler, *Zeolites* 3 (1983) 171.
- [28] D. Freude, T. Frohlich, M. Hunger, H. Pfeifer, G. Scheler, *Chem. Phys. Lett.* 98 (1983) 263.
- [29] G.J. Kühn, *J. Phys. Chem. Solids* 38 (1977) 1259.
- [30] A. Martin, U. Wolf, S. Nowak, B. Lucke, *Zeolites* 11 (1991) 85.
- [31] R.D. Shannon, K.H. Gardner, R.H. Stacey, G. Bergeret, P. Gallezot, A. Auroux, *J. Phys. Chem.* 89 (1985) 4778.
- [32] F.R. Chen, J.G. Davis, J.J. Fripiat, *J. Catal.* 133 (1992) 263.